Metalladiboranes of the iron subgroup: K[M(CO)4(.eta.2-B2H5)] (m-iron, ruthenium, osmium) and M'(.eta.5-C5H5) (CO)2(.eta.2-B2H5) (M' = iron, ruthenium). Analogs of metal-olefin complexes

Tim J. Coffy, George. Medford, Jeffrey. Plotkin, Gary J. Long, John C. Huffman, and Sheldon G. Shore

Organometallics, **1989**, 8 (10), 2404-2409• DOI: 10.1021/om00112a023 • Publication Date (Web): 01 May 2002

frequency set >2 ppm from all resonances. Spectra were obtained at 21 °C in interleaved blocks of 32 transients with four steady states per block for a total of at least 1216 transients. The acquisition time was 2.0 s, and the pulse delay was 6 s (selected to be at least three times the largest T_1 of interest: 1.7 s for H_γ; 1.4 s for H_β; 0.5–0.6 s for $H_{\alpha,\alpha'}$). Difference NOEs were calculated by substraction of the off-resonance spectrum from the η^5-C_5H_5-irradiated spectrum. Data were similarly acquired for **2a** with a pulse delay of 10 s; T_1 values: 1.1–1.3 s for $H_{\gamma,\gamma'}$; 3.2 s for H_β; 0.8 s for $H_{\alpha,\alpha'}$.

X-ray Crystal Structure of 2c. A sample of **2c** (0.078 g) was dissolved in toluene (2 mL), layered with heptane (7 mL), and kept at −20 °C for 7 days. Red prisms of **2c** formed, and the mother liquor was decanted. A crystal was mounted on a glass fiber, and axial photographs showed monoclinic symmetry. Unit-cell dimensions were obtained by least-squares refinement using 15 centered reflections for which $25° < 2\theta < 36°$. Data collection was carried out on a Nicolet R3m/E four-circle diffractometer as outlined in Table I.

Data reduction[27] included corrections for Lorentz and polarization effects. Systematic extinctions indicated the space group $P2_1/n$. A Patterson synthesis gave the rhenium position, and the remaining non-hydrogen atoms were located by difference maps. These were refined with anisotropic thermal parameters by blocked-cascade least squares, minimizing $\sum w\Delta^2$, with 101 parameters refined in each full-matrix block. Scattering factors were taken from the literature.[28] Empirical absorption corrections were based on the azimuthal scan data. Calculated hydrogen positions were used during refinement with a common refined isotropic thermal parameter.

Refinement behavior and difference maps indicated disorder of the allyl ligand. The subordinate orientation was related to the predominant orientation by rotations of ca. 27° and 170° about the Re–C1 and C1–C2 bonds, respectively, with some distortions from C1–C4 planarity to make the phenyl rings of the two orientations nearly coplanar. A disorder model giving approximate fit to the positions of difference map peaks was calculated from idealized geometry. The disorder model was introduced into the refinement with some constraints imposed on the subordinate orientation: isotropic refinement of carbon atoms; rigid group constraints for the phenyl ring; bond distances for C1–C2′, C2′–C3′, and C3′–C4′ set at the corresponding refined distances in the predominant orientation. The occupation factor for the subordinate orientation refined to 0.212 (2). Previously refined isotropic thermal parameters for the carbons of the subordinate orientation were fixed in the final cycles of refinement to facilitate convergence.

(27) All crystallographic calculations were performed on a Data General Eclipse computer using the SHELXTL program package by G. M. Sheldrick, Nicolet Analytical Instruments, Madison, WI, 1983.

(28) Cromer, D. T.; Waber, J. T. In *International Tables for X-ray Crystallography*; Ibers, J. A., Hamilton, W. C., Eds.; Kynoch: Birmingham, England, 1974; Vol. IV, pp 72–98, 149–150.

Acknowledgment. We thank the NIH for support of this research and A. Sopchik, A. Arif, and M. Dewey for assistance with high-field NMR spectra, X-ray data, and the Cambridge Crystallographic Data Base search.

Registry No. 2a, 97396-45-7; **2b**, 122295-31-2; **2c**, 122295-30-1; **3a** (isomer 1), 85955-92-6; **3a** (isomer 2), 85926-81-4; **3b**, 85926-83-6; **3c** (isomer 1), 115074-77-6; **3c** (isomer 2), 122442-00-6; (η^5-C_5H_5)Re(NO)(PPh_3)(H), 79919-58-7; 2-methallyl chloride, 107-05-1; cinnamyl chloride, 2687-12-9; allyl chloride, 107-05-1.

Supplementary Material Available: Tables of atomic coordinates, bond lengths and angles, and anisotropic thermal parameters for **2c** (3 pages); a listing of calculated and observed structure factors for **2c** (25 pages). Ordering information is given on any current masthead page.

Metalladiboranes of the Iron Subgroup: $K[M(CO)_4(\eta^2\text{-}B_2H_5)]$ (M = Fe, Ru, Os) and $M'(\eta^5\text{-}C_5H_5)(CO)_2(\eta^2\text{-}B_2H_5)$ (M′ = Fe, Ru). Analogues of Metal–Olefin Complexes

Tim J. Coffy,[†] George Medford,[†] Jeffrey Plotkin,[†] Gary J. Long,*[,‡] John C. Huffman,*[,§] and Sheldon G. Shore*[,†]

Department of Chemistry, The Ohio State University, 120 West 18th Avenue, Columbus, Ohio 43210, Department of Chemistry, University of Missouri—Rolla, Rolla, Missouri 65401, and Molecular Structure Center, Indiana University, Bloomington, Indiana 47405

Received March 29, 1989

The metal carbonylates $[M(CO)_4]^{2-}$ (M = Fe, Ru, Os) and $[(\eta^5\text{-}C_5H_5)M'(CO)_2]^-$ (M′ = Fe, Ru) react with $L{\cdot}BH_3$ (L = THF, Me_2O) to yield the metalladiborane complexes $[M(CO)_4(\eta^2\text{-}B_2H_5)]^-$ and $(\eta^5\text{-}C_5H_5)M'(CO)_2(\eta^2\text{-}B_2H_5)$. The molecular structure of $(\eta^5\text{-}C_5H_5)Fe(CO)_2(\eta^2\text{-}B_2H_5)$ was determined from single-crystal X-ray data. This structure can be described as that of a diborane(6) molecule with a $(\eta^5\text{-}C_5H_5)Fe(CO)_2$ unit replacing a bridge hydrogen. Distances and angles within the B_2H_5 unit are consistent with those observed for B_2H_6. Crystal data for $(\eta^5\text{-}C_5H_5)Fe(CO)_2(\eta^2\text{-}B_2H_5)$: space group *Pnam*, orthorhombic, a = 11.955 (3) Å, b = 6.425 (1) Å, c = 11.552 (3) Å, V = 887.44 Å^3, mol wt 204.04, ρ_{calcd} = 1.524 g/cm^3, for Z = 4. For Mo Kα 1355 unique reflections were collected at −174 °C over the range $5° < 2\theta < 55°$ with 1100 reflections greater than $2.33\sigma(I)$ used in the final refinement. R_F = 0.0254 and R_{wF} = 0.0303. Boron-11 and proton NMR spectra also indicate diborane-like structures for $[M(CO)_4(\eta^2\text{-}B_2H_5)]^-$ (M = Fe, Ru, Os) and $(\eta^5\text{-}C_5H_5)M'(CO)_2(\eta^2\text{-}B_2H_5)$. Mössbauer spectra as well as the X-ray diffraction data support a three-center, two-electron bond representation between the metal center and the two borons of the B_2H_5 moiety.

Introduction

The nucleophilic nature of transition-metal carbonylates is well established. Dessy and King[1] and later Pearson[2] determined relative nucleophilicities of selected transition-metal carbonylates through reactions with alkyl halides. Such carbonylates are expected to form addition

[†] Ohio State University.
[‡] University of Missouri—Rolla.
[§] Molecular Structure Center, Indiana University.

(1) Dessy, R. E.; Pohl, R. L.; King, R. B. *J. Am. Chem. Soc.* **1966**, *88*, 5121.
(2) Pearson, R. G.; Figdore, P. E. *J. Am. Chem. Soc.* **1980**, *102*, 1541.

0276-7333/89/2308-2404$01.50/0

compounds with Lewis acids. Parshall[3] provided the first report of the reaction of the Lewis acid BH_3 with the metal carbonylates $[M(CO)_5]^-$ (M = Mn, Re) and $[Mn(CO)_4PPh_3]^-$ to give the simple adducts $[(H_3B)Re(CO)_5]^-$ and $[(H_3B)Mn(CO)_4PPh_3]^-$. In preliminary reports[4] we described reactions of the highly nucleophilic anions $[Fe(CO)_4]^{2-}$ and $[(\eta^5\text{-}C_5H_5)Fe(CO)_2]^-$ with BH_3 to produce the metalladiboranes $[Fe(CO)_4(\eta^2\text{-}B_2H_5)]^-$ and $(\eta^5\text{-}C_5H_5)(CO)_2Fe(\eta^2\text{-}B_2H_5)$. More recently the photochemical synthesis of $(\eta^5\text{-}C_5H_5)_2HMo(\eta^2\text{-}B_2H_5)$ has been reported.[5] These compounds are diborane(6) analogues that contain an organometallic fragment occupying a bridge hydrogen site. They are also analogues of metal olefin complexes. Other types of B_2H_5 complexes have also been described: $(\eta^5\text{-}C_5H_5)Co_2(\mu\text{-}PPh_2)(B_2H_5)$,[6] 5:1′,2′-(1-$(\eta^5\text{-}C_5H_5)$Co-2,3-$(Me_3Si)_2C_2B_4H_3)(B_2H_5)$,[7] 2:1′,2′-$(B_5H_8)(B_2H_5)$,[8] 2:1′,2′-$(1,6\text{-}C_2B_4H_5)(B_2H_5)$,[8] and $Pt_2(PMe_2Ph)_2(B_2H_5)(B_6H_9)$.[32]

Herein we present details of the syntheses of the metalladiboranes $K_2[M(CO)_4(\eta^2\text{-}B_2H_5)]$ (M = Fe, Ru, Os) and $M'(\eta^5\text{-}C_5H_5)(CO)_2(\eta^2\text{-}B_2H_5)$ (M′ = Fe, Ru). Their properties including their NMR spectra, the X-ray structure of $Fe(\eta^2\text{-}C_5H_5)(CO)_2(\eta^2\text{-}B_2H_5)$, and the Mössbauer spectra of the iron–diborane complexes are also presented.

Experimental Section

General Data. All manipulations were performed in either a vacuum system or under an atmosphere of prepurified nitrogen. Tetrahydrofuran (THF) and dimethyl ether were distilled from sodium benzophenone ketyl immediately prior to use. $Os_3(CO)_{12}$ (Strem Chemical Co.) was used as received. $Fe_3(CO)_{12}$ (Strem) was recrystallized from hot CH_2Cl_2 prior to use. $Ru_3(CO)_{12}$ was prepared from $RuCl_3\cdot 3H_2O$ by a published procedure.[9] $K_2M(CO)_4$[10] (M = Fe, Ru, Os), B_2H_6,[11] and $K[M'(\eta^5\text{-}C_5H_5)(CO)_2]$ (M′ = Fe, Ru) were prepared from methods in the literature.[12,33] Bis(triphenylphosphine)nitrogen(1+) chloride, [PPN]Cl, and $[Ph_4As]Cl$ were heated to 150 °C under dynamic vacuum and stored under an atmosphere of dry nitrogen. Boron-11 NMR ($\delta(Et_2O\cdot BF_3)$ = 0.00 ppm) and proton NMR (δ(TMS) = 0.00 ppm) spectra were obtained on either a Bruker MSL-300 NMR spectrometer operating at 96.3 MHz and 300 MHz or a Bruker AM-250 NMR spectrometer operating at 80.2 MHz and 250 MHz, respectively.

$K[Fe(CO)_4(\eta^2\text{-}B_2H_5)]$. A 50-mL flask containing a Teflon coated magnetic stir bar was charged with 0.363 g (1.47 mmol) of $K_2[Fe(CO)_4]$. The flask was connected to a vacuum line extractor which was then evacuated on a high vacuum line. Dry THF was condensed (ca. 10 mL) into the flask at −78 °C (dry ice–2-propanol). The flask was then warmed to room temperature, and the THF solution was then stirred for 10–15 min to disperse the insoluble $K_2[Fe(CO)_4]$. A 3.15-mmol quantity of B_2H_6 was then condensed on top of the suspension at −196 °C. The reaction vessel was warmed to ambient temperature and stirred for 1 h. The solution was filtered leaving behind 0.102 g of KBH_4 precipitate representing a 94.5% yield. Volatiles, excess $THF\cdot BH_3$, and solvent were removed from the filtrate by evaporation under a dynamic vacuum through a U-trap maintained at −196 °C. No noncondensable gas was present. The remaining brown oil was alternately dissolved in diethyl ether and pumped on until solid brown $K[Fe(CO)_4(\eta^2\text{-}B_2H_5)]$ was attained (0.320 g, 93% yield based on $K_2[Fe(CO)_4]$). Infrared spectrum (THF): ν(B–H) 2450 (m), 2400 (m) cm^{-1}; ν(H–B–H) 1845 (w), 1655 (w) cm^{-1}; ν(CO) 2030 (w), 1943 (vs), 1927 (s) cm^{-1}. Anal. Calcd for $KC_4H_5B_2FeO_4$: C, 20.6; H, 2.16; B, 9.21; Fe, 23.9. Found: C, 20.7; H, 2.07; B, 8.93; Fe, 23.6.

A Study of the Stoichiometry of the Formation of $K[Fe(CO)_4(\eta^2\text{-}B_2H_5)]$. In a series of experiments the ratio of $THF\cdot BH_3$ to $K_2[Fe(CO)_4]$ was varied to determine the optimum yield of $K[Fe(CO)_4(\eta^2\text{-}B_2H_5)]$. Unreacted $THF\cdot BH_3$ was assayed by reaction with $P(CH_3)_3$ to form the $(CH_3)_3P\cdot BH_3$ adduct which was then weighed. The following procedure is an example of one trial.

The volatiles from the reaction of $K_2[Fe(CO)_4]$ with $THF\cdot BH_3$ (above) were condensed into a 50-mL flask containing a magnetic stirbar and a vacuum adapter. A 2.90-mmol quantity of $P(CH_3)_3$ was added, and the reaction mixture was stirred at room temperature for 1 h. The contents were fractionated by using a fractionation train with traps maintained at 0, −23, −78, and −196 °C. The $(CH_3)_3P\cdot BH_3$ was collected in the 0 °C trap. The $(CH_3)_3P\cdot BH_3$ was sublimed into a preweighed, removable U-trap which was then removed and weighed. The recovered $(CH_3)_3P\cdot BH_3$ (1.69 mmol) indicated that 4.60 mmol of BH_3 reacted with 1.47 mmol of $K_2[Fe(CO)_4]$ giving a ratio of $BH_3/K_2[Fe(CO)_4]$ = 3.13/1.00.

$K[Ru(CO)_4(\eta^2\text{-}B_2H_5)]$. $K[Ru(CO)_4(\eta^2\text{-}B_2H_5)]$ was prepared following the procedure for $K[Fe(CO)_4(\eta^2\text{-}B_2H_5)]$ with minor modifications. A typical reaction uses 0.430 g (1.48 mmol) of $K_2[Ru(CO)_4]$ and 2.26 mmol of B_2H_6, and the reaction time is 2 h. The yield is 350 mg (85% based on $K_2[Ru(CO)_4]$). Infrared spectrum (THF): ν(B–H) 2469 (m), 2426 (m) cm^{-1}; ν(H–B–H) 1850 (w), 1727 (w) cm^{-1}; ν(CO) 2056 (w), 2004 (vs), 1978 (s), 1956 (s) cm^{-1}. Anal. Calcd for $KC_4H_5B_2RuO_4\cdot 0.25THF$: C, 20.22; H, 2.38. Found: C, 20.86; H, 2.42.

$K[Os(CO)_4(\eta^2\text{-}B_2H_5)]$. $K[Os(CO)_4(\eta^2\text{-}B_2H_5)]$ was prepared following the procedure for $K[Fe(CO)_4(\eta^2\text{-}B_2H_5)]$ with minor modifications. A typical reaction uses 0.406 g (1.07 mmol) of $K_2[Os(CO)_4]$ and 1.62 mmol of B_2H_6, and the reaction time is 2 h. The yield is 370 mg (90% based on $K_2[Os(CO)_4]$). Infrared spectrum (THF): ν(B–H) 2433 (m), 2399 (m) cm^{-1}; ν(H–B–H) 1852 (w), 1688 (w) cm^{-1}; ν(CO) 2057 (w), 1961 (vs), 1921 (s) cm^{-1}. Anal. Calcd for $KC_4H_5B_2OsO_4\cdot 0.25THF$: C, 15.56; H, 1.82. Found: C, 15.03; H, 1.83.

$Fe(\eta^5\text{-}C_5H_5)(CO)_2(\eta^2\text{-}B_2H_5)$. In a controlled atmosphere box a 250-mL flask containing a Teflon-coated magnetic stir bar was charged with 1.080 g (5 mmol) of $K[Fe(\eta^5\text{-}C_5H_5)(CO)_2]$. The flask was connected to a vacuum line adapter and evacuated. Approximately 20 mL of Me_2O was distilled into the flask at −78 °C. The flask was then cooled to −196 °C, and 8.0 mmol of B_2H_6 was distilled into the vessel. The reaction mixture was warmed to −78 °C and stirred for 20 h. While the reaction flask was maintained at −78 °C, the solvent was removed via a U-trap maintained at −196 °C. The reaction flask was then warmed to 0 °C and evacuated for 20 min to remove unreacted $Me_2O\cdot BH_3$. After the flask was returned to the controlled atmosphere box, its contents were scraped into a water-cooled sublimator. The $Fe(\eta^5\text{-}C_5H_5)(CO)_2(\eta^2\text{-}B_2H_5)$ was sublimed at room temperature under vacuum for 30 h.[13] A crop of orange-yellow crystals condensed onto the coldfinger. The yield was 0.140 g (14% based on $K[(\eta^5\text{-}C_5H_5)Fe(CO)_2]$. Infrared spectrum ($CH_2Cl_2$): ν(B–H) 2492 (m), 2435 (m) cm^{-1}; ν(H–B–H) 1892 (w), 1698 (w) cm^{-1}; ν(CO) 2045 (vs), 1990 (vs) cm^{-1}. Mass Spectrum Calcd for $^1H_{10}{}^{11}B_2{}^{12}C_7{}^{16}O_2{}^{56}Fe$: 204.02158. Found: 204.02206.

$Ru(\eta^5\text{-}C_5H_5)(CO)_2(\eta^2\text{-}B_2H_5)$. In a controlled-atmosphere box 303 mg (1.16 mmol) of $K[(\eta^5\text{-}C_5H_5)Ru(CO)_2]$ was added to a 50-mL long-neck flask. The flask was equipped with a Teflon-coated magnetic stir bar and was connected to a vacuum line extractor. After evacuation, 5 mL of dry Me_2O was added to the flask at −78 °C and 2.50 mmol of B_2H_6 was added at −196 °C. The mixture was warmed to −38 °C (acetonitrile/N_2) and stirred for 4 h. During this time the color changed from an orange-yellow to a light yellow with a white precipitate. The white solid was identified by infrared spectroscopy as $K[BH_4]$. The solution was filtered through the

(3) Parshall, G. W. *J. Am. Chem. Soc.* **1964**, *86*, 361.
(4) (a) Medford, G.; Shore, S. G. *J. Am. Chem. Soc.* **1978**, *100*, 3953. (b) Plotkin, J. S.; Shore, S. G. *J. Organomet. Chem.* **1979**, *182*, C15.
(5) Grebnik, P. D.; Green, M. L. H.; Kelland, M. A.; Leach, J. B.; Mountford, P.; Stringer, G.; Walker, N. M.; Wong, L. L. *J. Chem. Soc., Chem. Commun.* **1988**, 799.
(6) Feilong, J.; Felhner, T. P.; Rheingold, A. L. *J. Organomet. Chem.* **1988**, *348*, C22.
(7) Briguglio, J. J.; Sneddon, L. G. *Organometallics* **1985**, *4*, 721.
(8) Corcoran, E. W.; Sneddon, L. G. *J. Am. Chem. Soc.* **1985**, *107*, 7446.
(9) Eady, C. R.; Jackson, P. F.; Johnson, B. F. G.; Lewis, J.; Malatesta, M. C.; McPartlin, M.; Nelson, W. J. H. *J. Chem. Soc., Dalton Trans.* **1980**, 383.
(10) Bhattacharryia, N. Ph.D. thesis, The Ohio State University, 1985.
(11) Toft, M. A.; Leach, J. B.; Himpsl, F. L.; Shore, S. G. *Inorg. Chem.* **1982**, *21*, 1952.
(12) Plotkin, J. S.; Shore, S. G. *Inorg. Chem.* **1981**, *20*, 284.

(13) The yield can be improved (ca. 30%) if the product is sublimed over longer periods of time (ca. 60 h).

Table I. Crystal Data for $Fe(\eta^5\text{-}C_5H_5)(CO)_2(\eta^2\text{-}B_2H_5)$

empirical formula	$FeB_2C_7O_2H_{10}$
fw	203.62
space group	*Pnam* (alternate setting for *Pnma*)
Z (molecules/cell)	4
temp, °C	−174
a, Å	11.955 (3)
b, Å	6.425 (1)
c, Å	11.552 (3)
V, unit cell Å^3	887.44
cryst dimens, mm	0.16 × 0.25 × 0.32
ρ_{calcd}, g cm^{-3}	1.524
μ, cm^{-1}	16.471
scan mode	ω–2θ
radiatn (λ, Å)	Mo Kα (0.710 730)
Min and max transmissn	0.7920, 0.7100
data collectn limits, deg 2θ	5–55
total no. of reflctns	5986
no. of unique intensities	1355 (R_{eq} = 0.024)
no. of reflctns used in structure refinement ($>2.33\sigma(I)$)	1100
$R_F = \sum\|\|F_o\| - \|F_c\|\|/\sum\|F_o\|$	0.0254
$R_{wF} = (\sum w(\|F_o\| - \|F_c\|)^2/\sum w\|F_o\|^2)^{1/2}$	0.0303
weighting scheme	$1/\sigma(\|F_o\|)^2$
goodness of fit for the last cycle	0.986

extractor by quickly tipping the extractor while the collection flask was cooled to −78 °C. The Me_2O and unreacted B_2H_6 were removed at −78 °C by pumping dynamically through a removable U-trap maintained at −196 °C. This left a yellow solid in the collection flask and the white $K[BH_4]$ on the frit. The solid was collected in the drybox and weighed. The yield was 187 mg (65% based on $K[(\eta^5\text{-}C_5H_5)Ru(CO)_2]$). Infrared spectrum ($CH_2Cl_2$): ν(B–H) 2488 (m), 2432 (m); ν(B–H–B) 1908 (w), 1722 (w); ν(CO) 2053 (vs), 2001 (vs) cm^{-1}.

X-ray Structure Determination of $Fe(\eta^2\text{-}C_5H_5)(CO)_2(\eta^2\text{-}B_2H_5)$. A pale yellow crystal obtained by sublimation under vacuum at room temperature was mounted on a previously described goniostat[14] and cooled to −174 °C. Lattice parameters were determined from a least-squares fit of angular data from 36 reflections, centered by using automated top/bottom and left/right slit assemblies. The structure was solved by a combination of direct methods (MULTAN78) and Fourier techniques. A summary of crystal data and intensity information is given in Table I.

Mössbauer Spectra. Spectra were obtained on a Harwell constant acceleration spectrometer which utilized a room-temperature rhodium-matrix source and was calibrated at room temperature with natural-α iron foil. The spectra were fit with symmetric quadrupole doublets by using standard least-squares fitting procedures.

Results and Discussion

Syntheses and Properties. LBH_3 (L = THF, Me_2O) reacts with the nucleophilic tetracarbonylates of the iron subgroup $[M(CO)_4]^{2-}$ (M = Fe, Ru, Os) and with $[M'(\eta^5\text{-}C_5H_5)(CO)_2]^-$ (M′ = Fe, Ru) to form metalladiboranes via reactions 1 and 2. In diethyl ether the reactions of

$$K_2[M(CO)_4] + 3THF{\cdot}BH_3 \rightarrow K[M(CO)_4(\eta^2\text{-}B_2H_5)] + K[BH_4] + 3THF \quad (1)$$

M = Fe, Ru, Os

$$K[M'(\eta^5\text{-}C_5H_5)(CO)_2] + 3Me_2O{\cdot}BH_3 \rightarrow M'(\eta^5\text{-}C_5H_5)(CO)_2(\eta^2\text{-}B_2H_5) + K[BH_4] + 3Me_2O \quad (2)$$

M′ = Fe, Ru

B_2H_6 with the carbonylates are very slow and typically are incomplete after several days. This is probably because the ether is too weak a base to produce an effective concentration of BH_3 by cleaving B_2H_6.

Relative stabilities of the $K[M(CO)_4(\eta^2\text{-}B_2H_5)]$ complexes decrease in the order Fe ≥ Os ≫ Ru. The iron and osmium salts are stable in THF for several days at room temperature in the absence of air, but the ruthenium complex is noticeably decomposed after 2 h. These salts are soluble in ethers and CH_3CN but are insoluble in CH_2Cl_2 and alkanes. Tetraphenylarsonium, and bis(triphenylphosphine)nitrogen(1+) salts are obtained from metathesis reactions in CH_2Cl_2 (reaction 3). Stabilities are enhanced by these large cations.

$$[M'R_4]Cl + K[M(CO)_4(\eta^2\text{-}B_2H_5)] \rightarrow [M'R_4][M(CO)_4(\eta^2\text{-}B_2H_5)] + KCl \quad (3)$$

$[M'R_4]$ = $[AsPh_4]$, $[NEt_4]$, [PPN]; M = Fe, Ru, Os

The complex $Fe(\eta^5\text{-}C_5H_5)(CO)_2(\eta^2\text{-}B_2H_5)$ can be handled in air for brief periods of time (several minutes). Under vacuum it shows no sign of decomposition after several hours, but it decomposes at elevated temperatures (ca. 50 °C). This compound readily sublimes under vacuum at room temperature. It is soluble in CH_2Cl_2, alkanes, and THF.

The compound $Ru(\eta^5\text{-}C_5H_5)(CO)_2(\eta^2\text{-}B_2H_5)$ is thermally unstable and decomposes in the solid state in less than 8 h. Samples of $Ru(\eta^5\text{-}C_5H_5)(CO)_2(\eta^2\text{-}B_2H_5)$ do not sublime unlike the analogous $Fe(\eta^5\text{-}C_5H_5)(CO)_2(\eta^2\text{-}B_2H_5)$, but the solubilities of the cyclopentadienyl analogues are similar.

Reaction Stoichiometry. The stoichiometry of reaction 1 was experimentally established. A 98% yield of $K[Fe(CO)_4(\eta^2\text{-}B_2H_5)]$ was obtained when the reactants were combined in a 3/1 $THF{\cdot}BH_3/K_2[Fe(CO)_4]$ ratio. Essentially all $THF{\cdot}BH_3$ added in excess of this ratio was recovered, while unreacted $K_2[Fe(CO)_4]$ and diminished yields of $K[Fe(CO)_4(\eta^2\text{-}B_2H_5)]$ were obtained when this ratio was less than 3/1. Quantitative recovery of $K[BH_4]$ revealed a 1/1 relationship between $K[BH_4]$ recovered and $K_2[Fe(CO)_4]$ added. $K[BH_4]$ was always formed in conjunction with the formation of $K[Fe(CO)_4(\eta^2\text{-}B_2H_5)]$. Even when the reaction ratio $K_2[Fe(CO)_4]/THF{\cdot}BH_3$ was larger than 1 and the reaction was followed in an NMR tube by means of ^{11}B NMR spectroscopy, no evidence was obtained for the formation of the simple adducts $K_2[Fe(CO)_4(BH_3)]$ and $K_2[Fe(CO)_4(BH_3)_2]$ as intermediates.

The driving force for reaction 1 is the precipitation of $K[BH_4]$ which is insoluble in THF, while $K[M(CO)_4(\eta^2\text{-}B_2H_5)]$ (M = Fe, Ru, Os) remains in solution. The reaction of $Na_2[M(CO)_4]$ with $THF{\cdot}BH_3$ is more complex because the $Na[BH_4]$ formed is soluble in THF and reacts with $THF{\cdot}BH_3$ to form THF-soluble $Na[B_3H_8]$ thereby producing a mixture of $Na[BH_4]$, $Na[B_3H_8]$, and $Na[M(CO)_4(\eta^2\text{-}B_2H_5)]$. Thus the isolation of pure $Na[M(CO)_4(\eta^2\text{-}B_2H_5)]$ is difficult to achieve.

Structure, Spectra, and Bonding. The molecular structure of $Fe(\eta^5\text{-}C_5H_5)(CO)_2(\eta^2\text{-}B_2H_5)$ was determined (Figure 1, Tables I and II) from single-crystal X-ray data obtained at −174 °C. The structure can be considered to be that of the diborane(6) molecule with one of the bridging protons replaced by $Fe(\eta^5\text{-}C_5H_5)(CO)_2$. A crystallographically imposed mirror plane passes through Fe(1), C(5), H(8), and H(11). Selected bond distances and angles are given in Tables III and IV. Distances and angles within the B_2H_5 unit are consistent with those observed for B_2H_6 (B–B = 1.776 Å).[15]

The values of B–B = 1.773 (8) Å, B–Fe_{av} = 2.217 (3) Å, B–Fe–B = 47.1 (2)°, and B–H–B = 88.5 (37)° for $Fe(\eta^5\text{-}C_5H_5)(CO)_2(\eta^2\text{-}B_2H_5)$ (Tables III and IV) are in excellent

(14) Huffman, J. C.; Lewis, L. N.; Caulton, K. G. *Inorg. Chem.* **1980**, *19*, 2755.

(15) Smith, H. W.; Lipscomb, W. N. *J. Chem. Phys.* **1965**, *43*, 1060.

Table II. Positional Parameters and Their Estimated Standard Deviations for $Fe(\eta^5\text{-}C_5H_5)(CO)_2(\eta^2\text{-}B_2H_5)$

atom	x	y	z	B, Å²
Fe(1)	0.41714 (2)	0.44151 (5)	0.75000[a]	1.2 (1)
B(2)	0.5804 (2)	0.3508 (4)	0.8269 (2)	2.6 (2)
C(3)	0.3847 (1)	0.2657 (3)	0.8629 (1)	1.7 (2)
O(4)	0.3583 (1)	0.1615 (2)	0.9379 (1)	2.4 (2)
C(5)	0.4654 (3)	0.7543 (4)	0.7500[a]	4.0 (2)
C(6)	0.4009 (2)	0.7139 (3)	0.8477 (2)	3.3 (2)
C(7)	0.2952 (2)	0.6497 (3)	0.8100 (2)	2.6 (2)
H(8)	0.656 (3)	0.3535 (7)	0.7500[a]	5.9 (9)[b]
H(9)	0.5849 (15)	0.200 (3)	0.8679 (17)	2.5 (4)[b]
H(10)	0.6047 (19)	0.474 (4)	0.8831 (20)	3.6 (5)[b]
H(11)	0.525 (3)	0.793 (7)	0.7500[a]	6.1 (11)[b]
H(12)	0.4239 (19)	0.722 (5)	0.9211 (22)	5.2 (6)[b]
H(13)	0.2357 (21)	0.602 (4)	0.8542 (20)	4.4 (6)[b]

[a] Fixed by symmetry. [b] Refined isotropically. Anisotropically refined atoms are given in the form of the isotropic equivalent thermal parameter defined as $(^4/_3)[a^2B(1,1) + b^2B(2,2) + c^2B(3,3) + ab(\cos\alpha\beta(1,2) + ac(\cos\beta)B(1,3) + bc(\cos\gamma)B(2,3)]$.

Table III. Selected Bond Distances (Å) and Their Estimated Standard Deviations for $Fe(\eta^5\text{-}C_5H_5)(CO)_2(\eta^2\text{-}B_2H_5)$

Fe(1)–C(3)	1.767 (3)	C(7)–C(7)	1.382 (6)
Fe(1)–C(5)	2.082 (5)	B(2)–B(2)	1.773 (8)
Fe(1)–C(6)	2.082 (3)	C(5)–H(11)	0.73 (5)
Fe(1)–C(7)	2.092 (3)	C(6)–H(12)	0.83 (4)
Fe(1)–B(2)	2.217 (3)	C(7)–H(13)	0.91 (4)
O(4)–C(3)	1.139 (3)	B(2)–H(8)	1.27 (4)
C(5)–C(6)	1.376 (4)	B(2)–H(9)	1.04 (4)
C(6)–C(7)	1.391 (5)	B(2)–H(10)	1.07 (4)

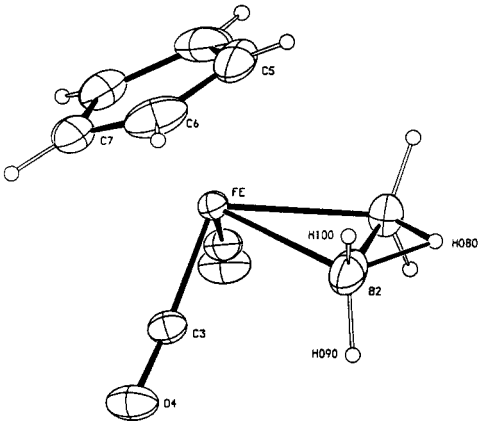

Figure 1. Molecular structure of $(\eta^5\text{-}C_5H_5)Fe(CO)_2(\eta^2\text{-}B_2H_5)$.

agreement with the related values (B–B = 1.773 (11) Å, $B\text{–}Fe_{av}$ = 2.207 (3) Å, B–Fe–B = 47.4 (3)°, and B–H–B = 88.5 (7)°) for $[N(n\text{-}C_4H_9)_4][Fe(CO)_4(\eta^2\text{-}B_7H_{12})]^-$. The anion $[Fe(CO)_4(\eta^2\text{-}B_7H_{12})]^-$ is an analogue of the complexes described in the present study in that the $Fe(CO)_4$ unit functions as a "pseudo bridge proton" in the B_7H_{12} unit.[16] The boron–iron distances in $Fe(\eta^5\text{-}C_5H_5)(CO)_2(\eta^2\text{-}B_2H_5)$ and $[N(n\text{-}C_4H_9)_4][Fe(CO)_4(\eta^2\text{-}B_7H_{12})]^-$ are somewhat longer than the 1.975 Å Fe–B single bond distance predicted from Pauling's[17] single bond radii. These "long" distances are consistent with three-center B–Fe–B bonding (Figure 2a) rather than two-center Fe–B bonds. If treated as separate two-center Fe–B bonds, these "long distances" imply bond orders of less than 1. The Mössbauer spectrum of the related complex $Fe(CO)_4(\eta^2\text{-}B_6H_{10})$ has been interpreted to infer three-center B–Fe–B bonding.[18] Also, the

(16) Mangion, M.; Clayton, W. R.; Hollander, O.; Shore, S. G. *Inorg. Chem.* **1977**, *16*, 2110.
(17) Pauling, L. *The Nature of the Chemical Bond*, 3rd ed.; Cornell University Press: Ithaca, NY, 1960.

Table IV. Selected Bond Angles (deg) and Their Estimated Standard Deviations for $Fe(\eta^5\text{-}C_5H_5)(CO)_2(\eta^2\text{-}B_2H_5)$

C(3)–Fe(1)–C(3)	95.1 (2)	Fe(1)–C(7)–C(6)	70.2 (2)
C(3)–Fe(1)–C(5)	132.4 (1)	Fe(1)–C(7)–C(7)	70.7 (1)
C(3)–Fe(1)–C(6)	96.8 (1)	C(6)–C(7)–C(7)	108.0 (2)
C(3)–Fe(1)–C(6)	155.7 (1)	Fe(1)–B(2)–B(2)	66.4 (1)
C(3)–Fe(1)–C(7)	120.0 (1)	Fe(1)–C(5)–H(11)	122 (4)
C(3)–Fe(1)–B(2)	74.4 (1)	C(6)–C(5)–H(11)	125.5 (3)
C(5)–Fe(1)–C(6)	38.6 (1)	Fe(1)–C(6)–H(12)	127 (3)
C(5)–Fe(1)–C(7)	64.7 (2)	C(5)–C(6)–H(12)	126.8 (2)
C(5)–Fe(1)–B(2)	90.7 (2)	C(7)–C(6)–H(12)	125.5 (2)
C(6)–Fe(1)–C(6)	65.1 (2)	Fe(1)–C(7)–H(13)	117.4 (2)
C(6)–Fe(1)–C(7)	65.0 (1)	C(6)–C(7)–H(13)	128.0 (2)
C(6)–Fe(1)–C(7)	38.9 (1)	C(7)–C(7)–H(13)	123.4 (2)
C(6)–Fe(1)–B(2)	120.9 (2)	Fe(1)–B(2)–H(8)	109.(2)
C(7)–Fe(1)–C(7)	38.6 (2)	Fe(1)–B(2)–H(9)	118.6 (2)
C(7)–Fe(1)–B(2)	130.1 (1)	Fe(1)–B(2)–H(10)	105.9 (2)
C(7)–Fe(1)–B(2)	155.3 (1)	B(2)–B(2)–H(8)	45.8 (2)
B(2)–Fe(1)–B(2)	47.1 (2)	B(2)–B(2)–H(9)	116.1 (2)
Fe(1)–C(3)–O(4)	175.6 (2)	B(2)–B(2)–H(10)	127.9 (2)
Fe(1)–C(5)–C(6)	70.7 (2)	H(8)–B(2)–H(9)	107 (3)
C(6)–C(5)–C(6)	109.0 (4)	H(8)–B(2)–H(10)	103 (3)
Fe(1)–C(6)–C(5)	70.7 (2)	H(9)–B(2)–H(10)	112.2 (2)
Fe(1)–C(6)–C(7)	70.9 (2)	B(2)–H(8)–B(2)	89 (4)
C(5)–C(6)–C(7)	107.6 (3)		

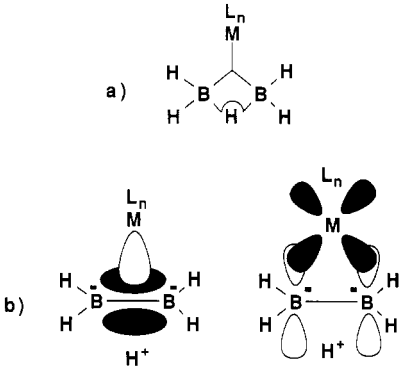

Figure 2. Possible bonding representations of the $(\eta^2\text{-}B_2H_5)$ ligand to the organometallic fragment in $ML_n(\eta^2\text{-}B_2H_5)$.

Mössbauer spectra of $K[Fe(CO)_4(\eta^2\text{-}B_2H_5)]$ and $Fe(\eta^5\text{-}C_5H_5)(CO)_2(\eta^2\text{-}B_2H_5)$ (described below) are consistent with three-center B–Fe–B bonds. Consideration of diborane(6) species in terms of the protonated double bond model of Pitzer[19] permits the iron–boron bonding mode to be likened, at least qualitatively, to the familiar Dewar–Chatt–Duncanson model[20,21] of metal–olefin bonding. This would correspond to the mixing of a π-bonding orbital with a vacant metal orbital and back-bonding from a filled metal orbital to the π^*-orbital (Figure 2b). The metal–boron bonding in $Fe(\eta^5\text{-}C_5H_5)(CO)_2(\eta^2\text{-}B_2H_5)$ has been analyzed from photoelectron spectroscopy and Fenske–Hall analysis.[22] The primary mode of bonding appears to be donation of electron density from the boron–boron bond to the vacant iron orbital, with little indication of back electron donation. For the tetracarbonylate complexes the metal is considered to be dsp^3 hybridized. In the analogous situation for $[Fe(CO)_4(\eta^2\text{-}B_7H_{12})]^-$ the three-center B–Fe–B bond occupies an equatorial site of the trigonal-bipyramidal ligand configuration around the Fe atom.[16] In the case of $Fe(\eta^5\text{-}C_5H_5)(CO)_2(\eta^2\text{-}B_2H_5)$ the iron can be considered to be d^2sp^3 hybridized.

(18) Davison, A.; Traficante, D. D.; Wreford, S. S. *J. Am. Chem. Soc.* **1974**, *96*, 2802.
(19) Pitzer, K. S. *J. Am. Chem. Soc.* **1945**, *67*, 1126.
(20) Dewar, M. J. S. *Bull. Soc. Chim. Fr.* **1951**, *18*, C71.
(21) Chatt, J.; Duncanson, L. A. *J. Chem. Soc.* **1953**, 2939.
(22) DeKock, R. L.; Deshmukh, P.; Fehlner, T. P.; Housecroft, C. E.; Plotkin, J. S.; Shore, S. G. *J. Am. Chem. Soc.* **1983**, *105*, 815.

Table V. NMR Data for the (η^2-B_2H_5) Complexes[a]

compound	$^{11}B\{^1H\}$[b]	$^1H\{^{11}B\}$	^{13}C	J_{BH}, Hz	J_{BHB}, Hz	J_{HH}, Hz
$CpFe(CO)_2(\eta^2\text{-}B_2H_5)$	−6.5[c]	5.01, 2.73, −5.33[c]		117	26	7.0
$CpRu(CO)_2(\eta^2\text{-}B_2H_5)$	−11.2[g]	5.39, 2.53, −6.12		119	36	6.9
$[Fe(CO)_4(\eta^2\text{-}B_2H_5)]^-$	−15.4	1.80, −5.17[e]	220	112	26	7.5
$[Ru(CO)_4(\eta^2\text{-}B_2H_5)]^-$	−18.4	1.56, −6.28	210	100	27[d,f]	7.0
$[Os(CO)_4(\eta^2\text{-}B_2H_5)]^-$	−24.0	1.45, −6.78	191	116	35[d,f]	7.8

[a] The NMR spectra of the anionic complexes are reported in THF-d_8 using the K^+ salt unless otherwise noted. The NMR shifts are in ppm. [b] $\delta(Et_2O{\cdot}BF_3) = 0.00$ ppm. [c] CD_2Cl_2. [d] CD_3CN. [e] $(CD_3)_2O$. [f] PPN^+ salt. [g] $CDCl_3$.

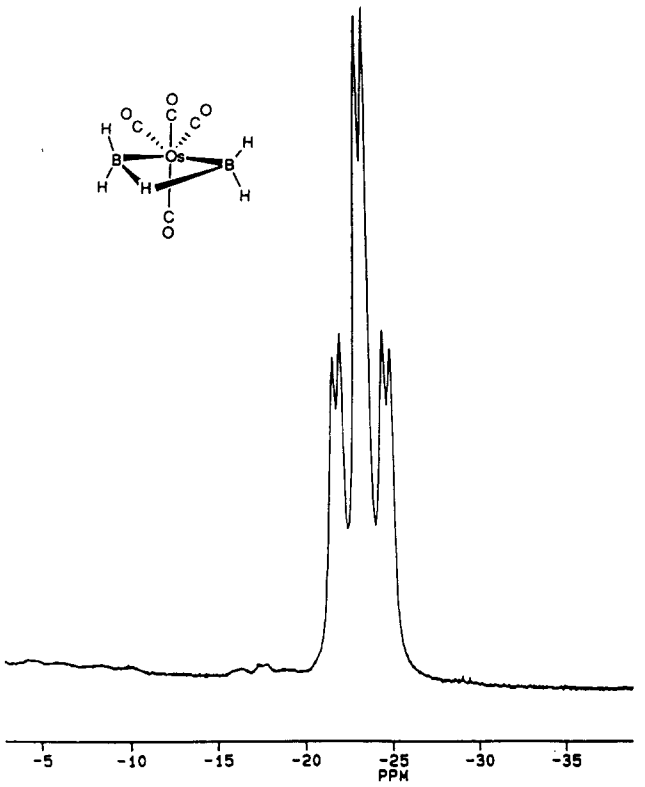

Figure 3. Boron-11 NMR spectrum of $[PPN][Os(CO)_4(\eta^2\text{-}B_2H_5)]$ in CD_3CN.

NMR spectral data are summarized in Table V. A typical ^{11}B NMR spectrum is shown in Figure 3. This spectrum is consistent with a structure in which the metal has replaced one of the proton bridges of the diborane(6), B_2H_6, molecule. The ^{11}B NMR spectrum, a triplet of doublets, indicates that two terminal hydrogens and a bridging hydrogen spin-couple with each of the equivalent boron atoms. The ^1H NMR spectrum reveals the presence of the terminal and bridging hydrogen atoms through a quartet (1:1:1:1) of relative area 4 and a broad upfield signal of relative area 1. Boron-11 spin decoupling causes the quartet resonance of the terminal hydrogens to collapse to a doublet, revealing ^1H–^1H spin coupling of the bridge hydrogen with the terminal hydrogens. Boron-11 spin decoupling also causes the bridging hydrogen signal to be resolved into a quintet, revealing the spin coupling of the four terminal hydrogens with the bridging hydrogen.

The resolution in the ^{11}B NMR spectrum of $[M(CO)_4(\eta^2\text{-}B_2H_5)]^-$ is a function of the counterion. Coupling of the bridge hydrogen with ^{11}B is observed only at elevated temperature (for M = Fe or Os), ca. 50 °C, for the K^+ salt. With a large complex anion such as $[PPN]^+$ the coupling is observed at room temperature (Figure 3). The ^{11}B and ^1H chemical shifts move upfield proceeding from iron to osmium in the iron subgroup. This trend might reflect the increasing electron-rich character of the metal. No evidence was observed for fluxional behavior involving interconversion of the terminal and bridge hydrogens over the temperature range in which the NMR spectra were observed (−80 to 80 °C).

Table VI. Mössbauer Effect Spectral Parameters[a]

compound	T, K	ΔE_Q	δ	Γ_1	ref
$[Fe(CO)_4(\eta^2\text{-}B_2H_5)]^-$	295	1.27	−0.23	0.31	this work
	78	1.33	−0.14	0.31	
	4.2	1.34	−0.13	0.33	
$H_2Fe(CO)_4$	80	0.55	−0.17		24
$Na_2[Fe(CO)_4]$	80	<0.18	−0.18		25
cis-$Fe(CO)_4I_2$	80	0.32	0.06		26
μ-$Fe(CO)_4B_6H_{10}$	300	1.71	−0.4		18
$(\eta^5\text{-}C_5H_5)Fe(CO)_2(\eta^2\text{-}B_2H_5)$	298	1.66	−0.004	0.24	this work
	78	1.68	0.072	0.27	
$(\eta^5\text{-}C_5H_5)Fe(CO)_2CN$	78	1.90	0.070	0.29	29
$(\eta^5\text{-}C_5H_5)Fe(CO)_2CH_3$	78	1.76	0.076	0.26	31

[a] All data in mm/s with the isomer shift relative to natural iron foil.

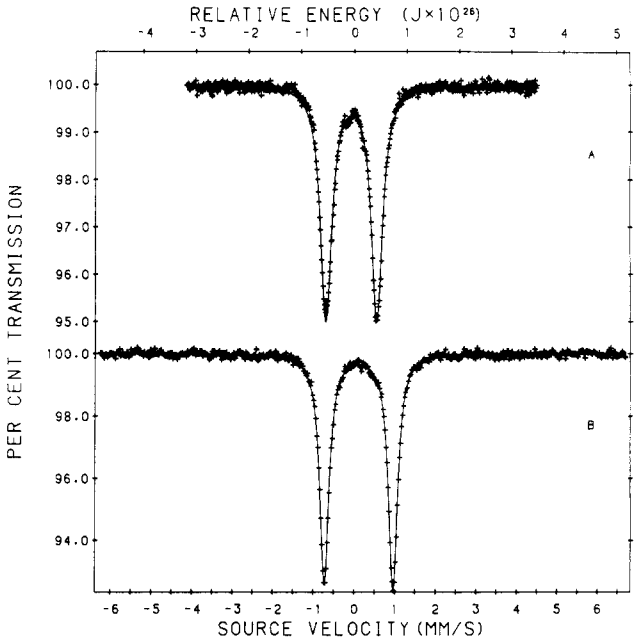

Figure 4. Mössbauer spectra of (a) $[Fe(CO)_4(\eta^2\text{-}B_2H_5)]^-$ and (b) $(\eta^5\text{-}C_5H_5)Fe(CO)_2(\eta^2\text{-}B_2H_5)$.

Carbon-13 NMR spectra of the compounds $[M(CO)_4(\eta^2\text{-}B_2H_5)]^-$ (M = Fe, Ru, Os) at 25 °C consist of single resonances (Table V), indicating equivalence of the carbonyls on the NMR time scale. The carbon-13 NMR spectra of $[M(CO)_4(\eta^2\text{-}B_2H_5)]^-$ (M = Fe, Ru, Os) were examined from room temperature to −120 °C and found to be invariant. Fluxional behavior is characteristic of many five-coordinate complexes.[23]

The Mössbauer effect spectral results for $K[Fe(CO)_4(\eta^2\text{-}B_2H_5)]$ and several related compounds are presented in Table VI.[18,24-26] The spectrum obtained at 78 K is

(23) Shapley, J. R.; Osborne, J. A. *Acc. Chem. Res.* **1973**, *6*, 305.
(24) Bancroft, G. M.; Mays, M. J.; Prater, B. E. *J. Chem. Soc. A* **1970**, 956.
(25) Mazak, R. A.; Collins, R. L. *J. Chem. Phys.* **1969**, *51*, 3220.

illustrated in Figure 4a. Very similar spectra were obtained at 295 and 4.2 K.

The low value of the Mössbauer effect isomer shift, observed in $K[Fe(CO)_4(\eta^2\text{-}B_2H_5)]$, provides further evidence in support of the single three-center B–Fe–B two-electron bonding mode. This bonding mode with its formal dsp^3 valence hybridization would be expected to have a smaller isomer shift than the alternate d^2sp^3 hybridization found in the two, two-center, two-electron bonding mode. The smaller isomer shift is expected for the dsp^3 hybridized bonding because of its high percentage s character and lower percentage d character relative to the d^2sp^3 bonding. Both of these factors favor an increased s-electron density at the iron nucleus and hence a low isomer shift. A low value for the isomer shift is also observed in $Fe(CO)_4(\eta^2\text{-}B_6H_{10})$ which is reported to contain[18] the three-center, two-electron bond. Alternatively the six-coordinate d^2sp^3 bonding yields a higher value for the isomer shift in *cis*-$Fe(CO)_4I_2$.

The three-center, two-electron bonding mode is also favored by the relatively large value of the quadrupole interaction observed in $K[Fe(CO)_4(\eta^2\text{-}B_2H_5)]$. In this bonding scheme, the iron(0) is five-coordinate trigonal bipyramidal, with the $B_2H_5^-$ species most likely occupying an equatorial position similar to that found in $Fe(CO)_4(\eta^2\text{-}C_2H_4)$[21] and in $Fe(CO)_4(\eta^2\text{-}CH_2CHCN)$.[27] In general iron(0) complexes exhibit large quadrupole interactions as a result of their formal d^8 electronic configuration which cannot lead to a cubic electronic environment.[28] In contrast, the iron(II) d^6 configuration and the iron(–II) d^{10} configuration can both lead to an essentially cubic electronic environment and a very small quadrupole interaction. Hence the large quadrupole interaction observed in $K[Fe(CO)_4(\eta^2\text{-}B_2H_5)]$ seems inconsistent with a six-coordinate pseudooctahedral coordination geometry in which there are two, two-center, Fe–B two-electron bonds in the $[Fe(CO)_4(\eta^2\text{-}B_2H_5)]^-$ anion. This conclusion is further supported by the large quadrupole interaction observed in $Fe(CO)_4(\eta^2\text{-}B_6H_{10})$[18] and the small value found in *cis*-$Fe(CO)_4I_2$.[26]

The Mössbauer effect spectrum of $Fe(\eta^5\text{-}C_5H_5)(CO)_2(\eta^2\text{-}B_2H_5)$ obtained at 78 K is shown in Figure 4b, and the resulting parameters are given in Table VI. The spectrum obtained at 298 K is essentially identical but with a smaller percent effect. Several papers[29–31] which have dealt with Mössbauer spectral properties of various $(\eta^5\text{-}C_5H_5)Fe(CO)_2$ derivatives have established a relationship between the relative σ plus π bonding between the iron and various ligands and the observed Mössbauer effect chemical isomer shift. Although it is not possible to resolve the σ- and π-bonding contributions to the chemical isomer shift, it is observed that the isomer shift is very sensitive to the composition of the derivative. This is the case both for halide and pseudohalide[29] derivatives and for various alkyl and silyl derivatives.[31] The similarities of the Mössbauer parameters for $Fe(\eta^5\text{-}C_5H_5)(CO)_2(\eta^2\text{-}B_2H_5)$, $Fe(\eta^5\text{-}C_5H_5)(CO)_2CN$, and $Fe(\eta^5\text{-}C_5H_5)(CO)_2CH_3$ are apparent in Table V. The very similar value of the isomer shift for these three compounds provides additional support for the proposal that the bonding between the iron and B_2H_5 group is best represented by one three-center, two-electron bond.[22] The alternative bonding scheme with the two two-center, two-electron Fe–B bonds seems much less reasonable. In the later case, one would expect to observe a chemical isomer shift somewhat lower than that found in the methyl or cyanide derivative. The three compounds also have similar values for the quadrupole interaction, but, as noted earlier,[30] it is difficult to draw electronic and structural conclusions from the values of the quadrupole interaction in these types of compounds.

Acknowledgment. We thank the National Science Foundation for support of this work through Grant CHE 88-00515. T.J.C. thanks B. P. America for a fellowship.

Registry No. $K[(Fe(CO)_4)(\eta^2\text{-}B_2H_5)]$, 67269-71-0; $K_2[Fe(CO)_4]$, 16182-63-1; B_2H_6, 19287-45-7; $K_2[Fe(CO)_4(\eta^2\text{-}B_2H_5)]$, 122019-24-3; $K[(Os(CO)_4)(\eta^2\text{-}B_2H_5)]$, 122019-25-4; $Fe(\eta^5\text{-}C_5H_5)(CO)_2(\eta^2\text{-}B_2H_5)$, 72576-54-6; $K_2[Os(CO)_4]$, 97295-89-1; $K_2[Ru(CO)_4]$, 110924-30-6; $K[Fe(\eta^5\text{-}C_5H_5)(CO)_2]$, 60039-75-0; ^{57}Fe, 14762-69-7.

Supplementary Material Available: A table of anisotropic thermal parameters (1 page); a listing of calculated and observed structure factor amplitudes (7 pages). Ordering information is given on any current masthead page.

(26) Vasudev, P.; Jones, C. H. W. *Canad. J. Chem.* **1973**, *51*, 405.
(27) Luxmore, A. R.; Truter, M. R. *Acta. Crystallogr.* **1962**, *15*, 1117.
(28) Parish, R. V. In *The Organic Chemistry of Iron*; Von Gustorf, E. A. K., Grevels, F. W., Fischler, I., Eds.; Academic Press: New York, 1978; Vol. I, p 175.
(29) Long, G. J.; Alway, D. G.; Barnett, K. W. *Inorg. Chem.* **1977**, *17*, 486.
(30) Johnson, B. V.; Ouseph, P. J.; Hsieh, J. S.; Dteinmetz, A. L.; Shade, J. E. *Inorg. Chem.* **1979**, *18*, 1796.
(31) Pannell, K. H.; Wu, C. C.; Long, G. J. *J. Organomet. Chem.* **1979**, *182*, C15.
(32) (a) Ahmad, R.; Crook, J. E.; Greenwood, N. N.; Kennedy, J. D.; McDonald, W. S. *J. Chem. Soc., Chem. Commun.* **1981**, 1019. (b) Ahmad, R.; Crook, J. E.; Greenwood, N. N.; Kennedy, J. D. *J. Chem. Soc., Dalton Trans.* **1986**, 2433.
(33) Doherty, N. M.; Knox, S. A. R. *Inorg. Synth.* **1989**, *25*, 179.